
A stabilised finite element method for the plate obstacle problem

Tom Gustafsson · Rolf Stenberg · Juha Videman

Received: date / Accepted: date

Abstract We introduce a stabilised finite element formulation for the Kirchhoff plate obstacle problem and derive both a priori and residual-based a posteriori error estimates using conforming C^1 -continuous finite elements. We implement the method as a Nitsche-type scheme and give numerical evidence for its effectiveness in the case of an elastic and a rigid obstacle.

Keywords Obstacle problem · Kirchhoff plate · stabilised FEM · a posteriori estimate · Nitsche's method

Mathematics Subject Classification (2010) 65N30 · 65K15 · 74S05

1 Introduction

The goal of this paper is to introduce a stabilised finite element method for the obstacle problem of clamped Kirchhoff plates and perform an a priori and a posteriori error analysis based on conforming finite element approximation of the displacement field.

Funding from Tekes (Decision number 3305/31/2015), the Finnish Cultural Foundation, the Portuguese Science Foundation (FCOMP-01-0124-FEDER-029408) and the Finnish Society of Science and Letters is greatly acknowledged.

Tom Gustafsson
Department of Mathematics and Systems Analysis, Aalto University, P.O. Box 11100, 00076 Aalto, Finland
E-mail: tom.gustafsson@aalto.fi

Rolf Stenberg
Department of Mathematics and Systems Analysis, Aalto University, P.O. Box 11100, 00076 Aalto, Finland
E-mail: rolf.stenberg@aalto.fi

Juha Videman
CAMGSD/Departamento de Matemática, Instituto Superior Técnico, Universidade de Lisboa, Av. Rovisco Pais 1, 1049-001 Lisboa, Portugal
E-mail: jvideman@math.tecnico.ulisboa.pt

To our knowledge, stabilised C^1 -continuous finite elements have not been previously analysed for fourth-order obstacle problems. Moreover, only a few articles exist on the a posteriori error analysis of fourth-order obstacle problems (cf. [17, 4]) and none on conforming C^1 -continuous finite elements, most probably due to the limited regularity of the underlying continuous problem. Here, we consider a stabilised method based on a saddle point formulation which introduces the contact force as an additional unknown (Lagrange multiplier). We establish an a priori estimate with minimal regularity assumptions and derive residual-based a posteriori error estimators. The Lagrange multiplier formulation has the advantage of providing an approximation for the contact force and the unknown contact domain. Moreover, it can easily be implemented as a Nitsche-type method with only the primal displacement variable as an unknown in the resulting linear system.

In a recent paper [18], we considered two families of finite element methods for a second-order obstacle problem using a Lagrange multiplier formulation for including the obstacle constraint. The first was a family of mixed finite element methods for which the discrete spaces need to satisfy the Babuška–Brezzi condition. This was achieved by using “bubble” degrees of freedom. The second was a family of stabilised methods for which the stability is guaranteed, for all finite element space pairs, by adding properly weighted residual terms to the discrete formulation. In the analysis of the stabilised formulation, we made use of recently developed tools for the Stokes problem [23].

In [18], the analysis was focused on the membrane obstacle problem. The approach followed is, however, quite general and should thus, up to some modifications, be extendable to other problems. In this paper, we consider conforming C^1 -continuous elements for clamped Kirchhoff plates constrained by a rigid or elastic obstacle. This kind of elements are rather complicated to work with and hence it does not seem reasonable to add artificial bubble degrees of freedom, in particular since the bubbles should belong to $H_0^2(K)$ at each element K . Therefore, we only address a stabilised formulation.

Numerical approximation of fourth-order obstacle-type problems has been previously studied in [14, 15, 21, 7, 5, 6, 4]. In [14, 15] the authors considered mixed finite element methods and presented general convergence theorems without convergence rates. In [21], it was shown that using the penalty method and piecewise quadratic elements, the method converges with the (suboptimal) rate of $h^{1/3}$ in the energy norm. Brenner et al. [7] made a unified a priori error analysis for classical conforming and non-conforming (C^1 -continuous and C^0 -continuous) finite element methods (see, e.g., [11]) as well as for the C^0 interior penalty methods and showed $\mathcal{O}(h)$ convergence rate for all methods in convex domains, see also [5, 6] for some generalisations. The only existing a posteriori analyses on fourth-order obstacle-type problems are due to Brenner et al. [4] and Gudi and Porwal [17], both performed on the C^0 interior penalty methods. In [17], the authors also derive a priori error estimates with minimal regularity assumptions using the techniques developed by Gudi in [16] much in the same spirit as we do here, see also [23, 18].

All the above mentioned papers address the problem with a rigid obstacle. For the plate bending problem with an elastic obstacle, we refer to [24] for general con-

vergence results in a mixed formulation and to [20] for optimal a priori estimates for conforming and non-conforming methods in the primal formulation.

The paper is organised as follows. In Section 2, we formulate the continuous problem and show its stability. In Section 3, we define the stabilised finite element method and establish a discrete stability estimate as well as a priori and a posteriori error estimates. In Section 4, we derive the corresponding Nitsche's method and discuss its implementation. Finally, in Section 5, we report results of numerical computations on two example problems. In Sections 2 and 3, we will shorten (or omit) derivations that can be inferred from our work on the Kirchhoff plate source problem [19] and on the membrane obstacle problem [18].

2 The continuous problem

Let us first recall the Kirchhoff–Love theory for thin plates (see, e.g., [12]). We denote the infinitesimal strain tensor as

$$\varepsilon(v) = \frac{1}{2}(\nabla v + \nabla v^T), \quad \forall v \in \mathbb{R}^2, \quad (2.1)$$

and consider the following isotropic linear elastic constitutive relationship, valid under plane stress conditions,

$$\mathbb{C}A = \frac{E}{1+\nu} \left(A + \frac{\nu}{1-\nu} (\text{tr}A)I \right), \quad \forall A \in \mathbb{R}^{2 \times 2}, \quad (2.2)$$

where E and ν are the Young's modulus and the Poisson ratio. Letting u stand for the deflection of the mid-surface of the plate and d for the plate's thickness, the curvature K and the bending moment M are defined as

$$K(u) = -\varepsilon(\nabla u), \quad M(u) = \frac{d^3}{12} \mathbb{C}K(u). \quad (2.3)$$

Assume that $\Omega \subset \mathbb{R}^2$ is a polygonal domain occupied by (the mid-surface of) the thin plate. Since our interest lies in the obstacle problem, we will consider only clamped boundary conditions. The strain energy corresponding to a displacement v of the plate is $\frac{1}{2}a(v, v)$, with

$$a(w, v) = \int_{\Omega} M(w) : K(v) \, dx. \quad (2.4)$$

The displacement is constrained by an obstacle, denoted by g , which is allowed to be either rigid or elastic. The energy resulting from contact with an elastic obstacle can be written as

$$\frac{1}{2\varepsilon} \int_{\Omega} (u - g)_-^2 \, dx, \quad (2.5)$$

where $\varepsilon > 0$ is the inverse of an appropriately scaled "spring constant" and

$$(u - g)_- = \min\{u - g, 0\}.$$

The loading consists of a distributed load $f \in L^2(\Omega)$ with the potential energy

$$l(v) = \int_{\Omega} f v \, dx. \quad (2.6)$$

The total energy thus reads as

$$I(v) = \frac{1}{2} a(v, v) + \frac{1}{2\varepsilon} \int_{\Omega} (v - g)_-^2 \, dx - l(v). \quad (2.7)$$

The space of kinematically admissible displacements is denoted by $V = H_0^2(\Omega)$. The displacement function u is thus obtained by minimising the energy, viz.

$$I(u) \leq I(v) \quad \forall v \in V, \quad (2.8)$$

or by solving the weak formulation: Find $u \in V$ such that

$$a(u, v) + \frac{1}{\varepsilon} ((u - g)_-, v) = l(v), \quad \forall v \in V, \quad (2.9)$$

where (\cdot, \cdot) is the usual $L^2(\Omega)$ inner product. The reaction force between the obstacle and the plate is given by

$$\lambda = -\frac{1}{\varepsilon} (u - g)_-. \quad (2.10)$$

In the limit $\varepsilon \rightarrow 0$, the obstacle becomes rigid and the problem reduces to that of constrained minimisation

$$u = \operatorname{argmin}_{v \in K} \left[\frac{1}{2} a(v, v) - l(v) \right], \quad (2.11)$$

with

$$K = \{ v \in H_0^2(\Omega) : v \geq g \text{ in } \Omega \}. \quad (2.12)$$

At the same time, the reaction force λ converges to the Lagrange multiplier associated with the constraint $v \geq g$.

The plate obstacle problem can be investigated based on the variational inequality formulation of problem (2.11) (see [21, 7, 5, 6]): Find $u \in K$ such that

$$a(u, v - u) \geq l(v - u), \quad \forall v \in K. \quad (2.13)$$

Here, we rewrite the problem using λ as an independent unknown to obtain a perturbed saddle point problem. From (2.10) it follows that the reaction force is non-negative, i.e. it belongs to the set

$$\Lambda = \{ \mu \in Q : \langle v, \mu \rangle \geq 0 \, \forall v \in V \text{ s.t. } v \geq 0 \text{ a.e. in } \Omega \}, \quad (2.14)$$

where the function space for the Lagrange multiplier is defined as

$$Q = \begin{cases} L^2(\Omega), & \text{if } \varepsilon > 0, \\ H^{-2}(\Omega), & \text{if } \varepsilon = 0, \end{cases} \quad (2.15)$$

and $\langle \cdot, \cdot \rangle : Q' \times Q \rightarrow \mathbb{R}$ denotes the duality pairing. We denote by $\|\cdot\|_k$ the usual norm in the Hilbert space $H^k(\Omega)$, $k \in \mathbb{N}$, let $\|\cdot\|_0$ be the norm in $L^2(\Omega)$ and equip the space $H^{-2}(\Omega) = [H_0^2(\Omega)]'$ with the norm

$$\|\xi\|_{-2} = \sup_{v \in V} \frac{\langle v, \xi \rangle}{\|v\|_2}. \quad (2.16)$$

Note that since the Lagrange multiplier in general belongs to $H^{-2}(\Omega)$ in case of a rigid obstacle, the obstacle g and the load f could be such that the contact domain reduces to a point (or a finite number of points).

Under appropriate smoothness assumptions, the solution to the plate bending problem over a rigid obstacle is in $H_{\text{loc}}^3(\Omega) \cap C^2(\Omega)$, in convex domains in $H^3(\Omega)$, cf. [13,9], but it cannot belong to $H^4(\Omega)$. The exact solutions given in [6,1] seem to indicate that the smoothness threshold is $C^{2,1/2}(\Omega)$ or $H^{7/2-\varepsilon}(\Omega)$, $\varepsilon > 0$. The solution to the clamped plate bending problem is more regular if the obstacle is elastic. In fact, assuming that the obstacle and the loading term are in $L^2(\Omega)$, the regularity of the solution is determined by the regularity of the source problem, cf. [20]. In particular, the solution belongs to $H^4(\Omega)$ if the interior angles of the domain Ω are smaller than $\approx 126.284^\circ$, cf. [3].

Formulation (2.9) can be written as: Find $u \in V$ and $\lambda \in \Lambda$ such that

$$a(u, v) - \langle v, \lambda \rangle = l(v), \quad \forall v \in V, \quad (2.17)$$

$$\langle u - g + \varepsilon \lambda, \mu - \lambda \rangle \geq 0, \quad \forall \mu \in \Lambda. \quad (2.18)$$

The stabilised finite element method exploits the strong form of the equations which we recall next. The static variables, the moment tensor M and the shear force Q , satisfy the following equilibrium equations which, due to the loading and the Lagrange multiplier, have to be interpreted in the sense of distributions

$$\operatorname{div} M(u) = Q(u), \quad -\operatorname{div} Q(u) - \lambda = l. \quad (2.19)$$

A simple elimination leads to the equation

$$\mathcal{A}(u) - \lambda = l, \quad (2.20)$$

with the biharmonic operator $\mathcal{A}(u)$ given by

$$\mathcal{A}(u) := D\Delta^2 u, \quad (2.21)$$

where D stands for the bending stiffness defined through

$$D = \frac{Ed^3}{12(1-\nu^2)}. \quad (2.22)$$

The strong form of problem (2.17)-(2.18) is thus: Find u and λ such that

$$\left. \begin{aligned} \mathcal{A}(u) - \lambda &= l \\ \lambda &\geq 0 \\ \frac{1}{\varepsilon}(u - g) + \lambda &\geq 0 \\ \lambda \left(\frac{1}{\varepsilon}(u - g) + \lambda \right) &= 0 \end{aligned} \right\} \text{ in } \Omega, \quad (2.23)$$

$$u = 0 \text{ and } \frac{\partial u}{\partial n} = 0 \text{ on } \partial\Omega. \quad (2.24)$$

Remark 1 *In case of a rigid obstacle, the first two equations in (2.23) remain the same and the last two reduce to*

$$u - g \geq 0 \text{ in } \Omega, \quad \lambda(u - g) = 0 \text{ in } \Omega.$$

Defining the bilinear and linear forms $\mathcal{B} : (V \times Q) \times (V \times Q) \rightarrow \mathbb{R}$ and $\mathcal{L} : V \times Q \rightarrow \mathbb{R}$ through

$$\mathcal{B}(w, \xi; v, \mu) = a(w, v) - \langle v, \xi \rangle - \langle w, \mu \rangle - \varepsilon \langle \xi, \mu \rangle, \quad (2.25)$$

$$\mathcal{L}(v, \mu) = (f, v) - \langle g, \mu \rangle, \quad (2.26)$$

the variational problem (2.17)-(2.18) can be reformulated as

Problem 1 (Variational formulation) *Find $(u, \lambda) \in V \times \Lambda$ such that*

$$\mathcal{B}(u, \lambda; v, \mu - \lambda) \leq \mathcal{L}(v, \mu - \lambda) \quad \forall (v, \mu) \in V \times \Lambda. \quad (2.27)$$

In the sequel, we will use the following norm in $V \times Q$

$$\| \! \| (w, \xi) \! \| = (\|w\|_2^2 + \|\xi\|_{-2}^2 + \varepsilon \|\xi\|_0^2)^{1/2}, \quad (2.28)$$

with respect to which the bilinear form \mathcal{B} is continuous. Moreover, we write $a \gtrsim b$ (or $a \lesssim b$) when $a \geq Cb$ (or $a \leq Cb$) for some positive constant C independent of the finite element mesh and of the parameter ε .

Theorem 1 (Continuous stability) *For every $(v, \mu) \in V \times Q$ there exists $w \in V$ such that*

$$\mathcal{B}(v, \mu; w, -\mu) \gtrsim \| \! \| (v, \mu) \! \| ^2 \quad \text{and} \quad \|w\|_2 \lesssim \| \! \| (v, \mu) \! \| . \quad (2.29)$$

Proof Define $p \in V$ through

$$a(p, q) = \langle q, \mu \rangle \quad \forall q \in V. \quad (2.30)$$

From the continuity of the bilinear form a it follows that

$$\frac{\langle q, \mu \rangle}{\|q\|_2} = \frac{a(p, q)}{\|q\|_2} \lesssim \|p\|_2 \quad \forall q \in V. \quad (2.31)$$

Since q is arbitrary, we have

$$\|\mu\|_{-2} = \sup_{q \in V} \frac{\langle q, \mu \rangle}{\|q\|_2} \lesssim \|p\|_2. \quad (2.32)$$

Moreover, the coercivity of the bilinear form a gives

$$\|p\|_2^2 \lesssim a(p, p) = \langle p, \mu \rangle \leq \|\mu\|_{-2} \|p\|_2 \Rightarrow \|p\|_2 \lesssim \|\mu\|_{-2}. \quad (2.33)$$

Choosing $w = v - p$, noting that

$$\begin{aligned} \mathcal{B}(v, \mu; v - p, -\mu) &= a(v, v) - \langle v, \mu \rangle + \langle p, \mu \rangle + \varepsilon \langle \mu, \mu \rangle \\ &= \frac{1}{2}(a(v, v) + a(p, p)) + \frac{1}{2}a(v - p, v - p) + a(p, p) + \varepsilon \langle \mu, \mu \rangle \end{aligned}$$

and applying inequalities (2.32) and (2.33) proves the result.

3 The finite element method

Let \mathcal{C}_h be a conforming shape regular triangulation of Ω which we assume to be polygonal. The finite element subspaces are

$$V_h \subset V, \quad Q_h \subset Q. \quad (3.1)$$

Moreover, we define

$$\Lambda_h = \{\mu_h \in Q_h : \mu_h \geq 0 \text{ in } \Omega\} \subset \Lambda. \quad (3.2)$$

Let us introduce the stabilised bilinear and linear forms \mathcal{B}_h and \mathcal{L}_h by

$$\mathcal{B}_h(w, \xi; v, \mu) = \mathcal{B}(w, \xi; v, \mu) - \alpha \sum_{K \in \mathcal{C}_h} h_K^4 (\mathcal{A}(w) - \xi, \mathcal{A}(v) - \mu)_K, \quad (3.3)$$

$$\mathcal{L}_h(v, \mu) = \mathcal{L}(v, \mu) - \alpha \sum_{K \in \mathcal{C}_h} h_K^4 (f, \mathcal{A}(v) - \mu)_K, \quad (3.4)$$

where $\alpha > 0$ is the stabilisation parameter.

Problem 2 (The stabilised method) Find $(u_h, \lambda_h) \in V_h \times \Lambda_h$ such that

$$\mathcal{B}_h(u_h, \lambda_h; v_h, \mu_h - \lambda_h) \leq \mathcal{L}_h(v_h, \mu_h - \lambda_h) \quad \forall (v_h, \mu_h) \in V_h \times \Lambda_h. \quad (3.5)$$

For the existence of a unique solution to Problem 2, see, e.g., [8].

Let us define the mesh-dependent norms

$$\|\xi_h\|_{-2,h}^2 = \sum_{K \in \mathcal{C}_h} h_K^4 \|\xi_h\|_{0,K}^2, \quad (3.6)$$

$$\| (w_h, \xi_h) \|_h^2 = \|w_h\|_2^2 + \|\xi_h\|_{-2}^2 + \|\xi_h\|_{-2,h}^2 + \varepsilon \|\xi_h\|_0^2, \quad (3.7)$$

and recall the following estimate.

Lemma 1 (Inverse inequality) *There exists $C_I > 0$ such that*

$$C_I \|\mathcal{A}(w_h)\|_{-2,h}^2 \leq a(w_h, w_h) \quad \forall w_h \in V_h. \quad (3.8)$$

The inverse estimate of the following lemma is valid in an arbitrary piecewise polynomial finite element space Q_h .

Lemma 2 *It holds that*

$$\|\xi_h\|_{-2,h} \lesssim \|\xi_h\|_{-2} \quad \forall \xi_h \in Q_h. \quad (3.9)$$

Proof Let $b_K \in P_6(K)$ be the sixth order bubble function

$$b_K = (\lambda_{1,K} \lambda_{2,K} \lambda_{3,K})^2, \quad (3.10)$$

where $\lambda_{j,K}, j \in \{1, 2, 3\}$, denote the barycentric coordinates for $K \in \mathcal{C}_h$, and define the auxiliary space

$$W_h = \{v_h \in H_0^2(\Omega) \mid v_h|_K = b_K \xi_h|_K, \xi_h \in Q_h\}.$$

Given $\xi \in Q_h$, we now define $v_h \in W_h$ by

$$v_h|_K = h_K^4 b_K \xi_h|_K, \quad K \in \mathcal{C}_h.$$

From the norm equivalence and the inverse estimates, it follows that

$$(v_h, \xi_h) \gtrsim \|\xi_h\|_{-2,h}^2$$

and

$$\|v_h\|_2 \lesssim |v_h|_2 \lesssim \|\xi_h\|_{-2,h}.$$

Therefore

$$\|\xi_h\|_{-2,h} \lesssim \frac{(v_h, \xi_h)}{\|v_h\|_2}$$

and the assertion follows from the definition of the negative norm (2.16).

For the proof of the following result, we refer to [18] (with minor modifications).

Lemma 3 *There exist positive constants C_1 and C_2 such that*

$$\sup_{v_h \in V_h} \frac{\langle v_h, \xi_h \rangle}{\|v_h\|_2} \geq C_1 \|\xi_h\|_{-2} - C_2 \|\xi_h\|_{-2,h} \quad \forall \xi_h \in Q_h. \quad (3.11)$$

Theorem 2 (Discrete stability) *Suppose that $0 < \alpha < C_I$. It holds: for all $(v_h, \mu_h) \in V_h \times Q_h$ there exists $w_h \in V_h$ such that*

$$\mathcal{B}_h(v_h, \mu_h; w_h, -\mu_h) \gtrsim \|(v_h, \mu_h)\|_h^2 \quad \text{and} \quad \|(w_h, -\mu_h)\|_h \lesssim \|(v_h, \mu_h)\|_h. \quad (3.12)$$

Proof In view of the inverse inequality (3.8), it holds

$$\begin{aligned} & \mathcal{B}_h(v_h, \boldsymbol{\mu}_h; v_h, -\boldsymbol{\mu}_h) \\ &= a(v_h, v_h) + \varepsilon \|\boldsymbol{\mu}_h\|_0^2 - \alpha \|\mathcal{A}(v_h)\|_{-2,h}^2 + \alpha \|\boldsymbol{\mu}_h\|_{-2,h}^2 \\ &\geq (1 - \alpha C_I^{-1}) a(v_h, v_h) + \min\{1, \alpha\} (\|\boldsymbol{\mu}_h\|_{-2,h}^2 + \varepsilon \|\boldsymbol{\mu}_h\|_0^2). \end{aligned} \quad (3.13)$$

Let $q_h \in V_h$ be the function corresponding to the supremum in Lemma 3, scaled in such a way that $\|q_h\|_2 = \|\boldsymbol{\mu}_h\|_{-2}$. Then

$$\begin{aligned} & \mathcal{B}_h(v_h, \boldsymbol{\mu}_h; -q_h, 0) \\ &= -a(v_h, q_h) + \langle q_h, \boldsymbol{\mu}_h \rangle + \alpha \sum_{K \in \mathcal{C}_h} h_K^4 (\mathcal{A}(v_h) - \boldsymbol{\mu}_h, \mathcal{A}(q_h))_{0,K} \\ &\geq -\|v_h\|_2 \|q_h\|_2 + C_1 \|\boldsymbol{\mu}_h\|_{-2} \|q_h\|_2 - C_2 \|\boldsymbol{\mu}_h\|_{-2,h} \|q_h\|_2 \\ &\quad - \alpha (\|\mathcal{A}(v_h)\|_{-2,h} + \|\boldsymbol{\mu}_h\|_{-2,h}) \|\mathcal{A}(q_h)\|_{-2,h}. \end{aligned} \quad (3.14)$$

Using again the inverse inequality (3.8), Young's inequality and the continuity of the bilinear form a , we conclude that

$$\mathcal{B}_h(v_h, \boldsymbol{\mu}_h; -q_h, 0) \geq C_3 \|\boldsymbol{\mu}_h\|_{-2}^2 - C_4 (a(v_h, v_h) + \|\boldsymbol{\mu}_h\|_{-2,h}^2). \quad (3.15)$$

Finally, taking $w_h = v_h - \delta q_h$ and using estimates (3.13) and (3.15), together with the coercivity of a and the assumption $0 < \alpha < C_I$, proves the stability bound after $\delta > 0$ is chosen small enough.

The estimate $\| \langle w_h, -\boldsymbol{\mu}_h \rangle \| \lesssim \| \langle v_h, \boldsymbol{\mu}_h \rangle \|$ is trivial and the same bound in the discrete norm follows from the inverse estimate (3.9).

Remark 2 Note that the discrete stability bounds (3.12) are also valid in the continuous norm $\| \langle \cdot, \cdot \rangle \|$.

In the sequel, our functions may belong to the space $H^{-2}(\omega)$, $\omega \subset \Omega$, equipped with the norm

$$\|\boldsymbol{\mu}\|_{-2,\omega} = \sup_{z \in H_0^2(\omega)} \frac{\langle z, \boldsymbol{\mu} \rangle}{\|z\|_{2,\omega}}. \quad (3.16)$$

This means that if $w \in H_0^2(\Omega)$ is such that $w|_\omega \in H_0^2(\omega)$ and $w = 0$ in $\Omega \setminus \omega$, we can write

$$\langle w, \boldsymbol{\mu} \rangle \leq \|\boldsymbol{\mu}\|_{-2,\omega} \|w\|_{2,\omega}, \quad \forall \boldsymbol{\mu} \in H^{-2}(\omega). \quad (3.17)$$

Let $f_h \in V_h$ be the L^2 projection of f and define the data oscillation as

$$\text{osc}_K(f) = h_K^2 \|f - f_h\|_{0,K}, \quad (3.18)$$

$$\text{osc}(f)^2 = \sum_{K \in \mathcal{C}_h} \text{osc}_K(f)^2. \quad (3.19)$$

Furthermore, we recall the following integration by parts formula (cf. [12]), valid in any domain $R \subset \Omega$

$$\begin{aligned} a_R(w, v) &= \int_R \mathcal{A}(w) v \, dx + \int_{\partial R} Q_n(w) v \, ds \\ &\quad - \int_{\partial R} \left(M_{nn}(w) \frac{\partial v}{\partial n} + M_{ns}(w) \frac{\partial v}{\partial s} \right) ds. \end{aligned} \quad (3.20)$$

where we have used the shorthand notation

$$a_R(w, v) = \int_R M(w) : K(v) \, dx,$$

and defined the normal shear force and the normal and twisting moments through

$$\begin{aligned} Q_n(w) &= Q(w) \cdot n, \quad M_{nn}(w) = n \cdot M(w)n, \\ M_{ns}(w) &= M_{sn}(w) = s \cdot M(w)n, \end{aligned}$$

with n and s denoting the normal and tangential directions at ∂R . Integrating by parts on a smooth subset $S \subset R$ we get

$$\int_S Q_n(w)v \, ds - \int_S M_{ns}(w) \frac{\partial v}{\partial s} \, ds = \int_S V_n(w) \, ds - \Big|_a^b M_{ns}(w)v, \quad (3.21)$$

where a and b are the endpoints of S and the quantity

$$V_n(w) = Q_n(w) + \frac{\partial M_{ns}(w)}{\partial s} \quad (3.22)$$

is called the *Kirchhoff shear force* (cf. [12]). Denote by $\omega_E = K_1 \cup K_2$ the pair of triangles sharing an edge E and define jumps in the normal moment and the shear force over E through

$$\begin{aligned} \llbracket M_{nn}(v) \rrbracket_E &= M_{nn}(v) - M_{n'n'}(v) \\ \llbracket V_n(v) \rrbracket_E &= V_n(v) + V_{n'}(v). \end{aligned}$$

where n and n' stand for the outward normals to K_1 and K_2 , respectively.

We will need the following lemma in proving the a priori and a posteriori estimates. We will sketch its proof and refer to [19] for more details.

Lemma 4 *For all $v_h \in V_h$ and $\mu_h \in Q_h$ it holds that*

$$h_K^2 \|\mathcal{A}(v_h) - \mu_h - f\|_{0,K} \lesssim \|u - v_h\|_{2,K} + \|\lambda - \mu_h\|_{-2,K} + \text{osc}_K(f), \quad (3.23)$$

$$h_E^{1/2} \|\llbracket M_{nn}(v_h) \rrbracket\|_{0,E} \lesssim \|u - v_h\|_{2,\omega_E} + \|\lambda - \mu_h\|_{-2,\omega_E} + \sum_{K \subset \omega_E} \text{osc}_K(f), \quad (3.24)$$

$$h_E^{3/2} \|\llbracket V_n(v_h) \rrbracket\|_{0,E} \lesssim \|u - v_h\|_{2,\omega_E} + \|\lambda - \mu_h\|_{-2,\omega_E} + \sum_{K \subset \omega_E} \text{osc}_K(f). \quad (3.25)$$

Proof Recall from (3.10) the sixth order bubble $b_K \in P_6(K)$ and let

$$z_K = b_K h_K^4 (\mathcal{A}(v_h) - \mu_h - f),$$

for every $(v_h, \mu_h) \in V_h \times \Lambda_h$. Testing with z_K in the continuous variational problem (2.17) gives the identity

$$a_K(u, z_K) - \langle z_K, \lambda \rangle = (f, z_K)_K.$$

We have

$$\begin{aligned}
& h_K^4 \|\mathcal{A}(v_h) - \mu_h - f_h\|_{0,K}^2 \\
& \lesssim h_K^4 \|\sqrt{b_K}(\mathcal{A}(v_h) - \mu_h - f_h)\|_{0,K}^2 \\
& = (\mathcal{A}(v_h) - \mu_h - f_h, z_K)_K \\
& = (\mathcal{A}(v_h) - \mu_h, z_K)_K - (f, z_K)_K + (f - f_h, z_K)_K \\
& = a_K(v_h - u, z_K) + \langle z_K, \lambda - \mu_h \rangle + (f - f_h, z_K)_K.
\end{aligned} \tag{3.26}$$

The bound (3.23) follows from the continuity of a , Cauchy–Schwarz and inverse inequalities and from inequality (3.17).

Following [17], see also [19], we let $\omega_E = K_1 \cup K_2$ and define an auxiliary function $w = p_1 p_2 p_3$ in such a way that

- p_1 is the extension of $\llbracket M_{nn}(v_h) \rrbracket$ to ω_E such that $\frac{\partial p_1}{\partial n_E} = 0$;
- p_2 is the eight order bubble that, together its first order derivatives, vanishes at $\partial\omega_E$ and equals to one at the midpoint of E ;
- p_3 is the linear polynomial that is zero on E and satisfies $\frac{\partial p_3}{\partial n_E} = 1$.

Outside of ω_E , w is extended by zero, see [19] for more details. From the construction of w and formula (3.20), it follows that

$$\begin{aligned}
\|\llbracket M_{nn}(v_h) \rrbracket\|_{0,E}^2 & \lesssim (M_{nn}(v_h), \frac{\partial w}{\partial n_E})_E \\
& = -a_{\omega_E}(v_h, w) + (\mathcal{A}(v_h), w)_{\omega_E} \\
& = a_{\omega_E}(u - v_h, w) + (\mathcal{A}(v_h) - \mu_h - f, w)_{\omega_E} + \langle w, \mu_h - \lambda \rangle.
\end{aligned}$$

Bound (3.24) can now be established using the continuity of the bilinear form a , the Cauchy–Schwarz and inverse inequalities, a scaling argument and inequalities (3.17) and (3.23), see [18] and [19] for similar considerations.

The proof of (3.25) is similar except for the construction of the auxiliary function. We choose w' as a function defined on a subset of ω_E , consisting of two smaller triangles K'_1 and K'_2 , symmetric with respect to the edge E , and write $\omega'_E = K'_1 \cup K'_2$, $K'_j \subset K_j$, $j \in \{1, 2\}$. Then we define $w' = p'_1 p'_2$ where

- p'_1 is an extension of $\llbracket V_n(v_h) \rrbracket$ to ω'_E such that $\frac{\partial p'_1}{\partial n_E} = 0$;
- p'_2 is the eight order bubble that, together its first order derivatives, vanishes on $\partial\omega'_E$ and equals to one at the midpoint of E .

Note that now due to symmetry $\frac{\partial w'}{\partial n_E}|_E = 0$. Now, recalling identities (3.20) and (3.21), and integrating in parts in the last term on its right-hand side (cf. [19]), we obtain

$$\begin{aligned}
\|\llbracket V_n(v_h) \rrbracket\|_{0,E}^2 & \lesssim (V_n(v_h), w')_E \\
& = -a_{\omega'_E}(v_h, w') + (\mathcal{A}(v_h), w')_{\omega'_E} \\
& = a_{\omega'_E}(u - v_h, w') + (\mathcal{A}(v_h) - \mu_h - f, w')_{\omega'_E} + \langle w', \mu_h - \lambda \rangle,
\end{aligned}$$

from which estimate (3.25) can be concluded as the final step for bound (3.24).

Theorem 3 (A priori estimate) *It holds that*

$$\begin{aligned} & \|\!(u - u_h, \lambda - \lambda_h)\!\| \\ & \lesssim \inf_{\substack{v_h \in V_h, \\ \mu_h \in \Lambda_h}} \left(\|\!(u - v_h, \lambda - \mu_h)\!\| + \sqrt{\langle u - g + \varepsilon \lambda, \mu_h \rangle} \right) + \text{osc}(f). \end{aligned} \quad (3.27)$$

Proof Let $(v_h, \mu_h) \in V_h \times Q_h$ be arbitrary and assume that $w_h \in V_h$ is the function corresponding to $(u_h - v_h, \lambda_h - \mu_h)$ in the discrete stability estimate (3.12) expressed in the continuous norm $\|\!(\cdot, \cdot)\!\|$, see Remark 2. The problem statement then implies that

$$\begin{aligned} \|\!(u_h - v_h, \lambda_h - \mu_h)\!\|^2 & \lesssim \mathcal{B}_h(u_h - v_h, \lambda_h - \mu_h; w_h, \mu_h - \lambda_h) \\ & \lesssim \mathcal{L}_h(w_h, \mu_h - \lambda_h) - \mathcal{B}(v_h, \mu_h, w_h, \mu_h - \lambda_h) \\ & \quad + \alpha \sum_{K \in \mathcal{C}_h} h_K^4 (\mathcal{A}(v_h) - \mu_h, \mathcal{A}(w_h) + \lambda_h - \mu_h)_K \\ & = \mathcal{B}(u - v_h, \lambda - \mu_h; w_h, \mu_h - \lambda_h) + \langle u - g + \varepsilon \lambda, \mu_h - \lambda_h \rangle \\ & \quad + \alpha \sum_{K \in \mathcal{C}_h} h_K^4 (\mathcal{A}(v_h) - \mu_h - f, \mathcal{A}(w_h) + \lambda_h - \mu_h)_K. \end{aligned}$$

Let us bound separately each term on the right hand side. The continuity of the bilinear form \mathcal{B} and the second estimate in (3.12) yield for the first term

$$\begin{aligned} \mathcal{B}(u - v_h, \lambda - \mu_h; w_h, \mu_h - \lambda_h) & \lesssim \|\!(u - v_h, \lambda - \mu_h)\!\| \|\!(w_h, \mu_h - \lambda_h)\!\| \\ & \lesssim \|\!(u - v_h, \lambda - \mu_h)\!\| \|\!(u_h - v_h, \lambda_h - \mu_h)\!\|. \end{aligned}$$

For the second term we obtain

$$\langle u - g + \varepsilon \lambda, \mu_h - \lambda_h \rangle \leq \langle u - g + \varepsilon \lambda, \mu_h - \lambda \rangle = \langle u - g + \varepsilon \lambda, \mu_h \rangle.$$

The third term is bounded as follows

$$\begin{aligned} & \sum_{K \in \mathcal{C}_h} h_K^4 (\mathcal{A}(v_h) - \mu_h - f, \mathcal{A}(w_h) + \lambda_h - \mu_h)_K \\ & \leq \left(\sum_{K \in \mathcal{C}_h} h_K^4 \|\mathcal{A}(v_h) - \mu_h - f\|_{0,K}^2 \right)^{1/2} \left(\sum_{K \in \mathcal{C}_h} h_K^4 \|\mathcal{A}(w_h)\|_{0,K}^2 \right)^{1/2} \\ & \quad + \left(\sum_{K \in \mathcal{C}_h} h_K^4 \|\mathcal{A}(v_h) - \mu_h - f\|_{0,K}^2 \right)^{1/2} \left(\sum_{K \in \mathcal{C}_h} h_K^4 \|\lambda_h - \mu_h\|_{0,K}^2 \right)^{1/2} \\ & \lesssim (\|u - v_h\|_2 + \|\lambda - \mu_h\|_{-2} + \text{osc}(f)) \left(\sqrt{a(w_h, w_h)} + \|\lambda_h - \mu_h\|_{-2,h} \right) \\ & \lesssim (\|\!(u - v_h, \lambda - \mu_h)\!\| + \text{osc}(f)) \|\!(u_h - v_h, \lambda_h - \mu_h)\!\|, \end{aligned}$$

where we have used (3.23), the second estimate in (3.12) and the inverse inequalities (3.8) and (3.9).

To derive a posteriori error bounds, we define the local residual estimators

$$\eta_K^2 = h_K^4 \|\mathcal{A}(u_h) - \lambda_h - f\|_{0,K}^2, \quad (3.28)$$

$$\eta_E^2 = h_E^3 \|\llbracket V_n(u_h) \rrbracket\|_{0,E}^2 + h_E \|\llbracket M_{nn}(u_h) \rrbracket\|_{0,E}^2, \quad (3.29)$$

and the corresponding global residual estimator

$$\eta^2 = \sum_{K \in \mathcal{C}_h} \eta_K^2 + \sum_{E \in \mathcal{E}_h^I} \eta_E^2, \quad (3.30)$$

where \mathcal{E}_h^I denotes the set of interior edges in the mesh. An additional global estimator S , due to the unknown location of the contact boundary, is defined through

$$S^2 = ((u_h - g + \varepsilon \lambda_h)_+, \lambda_h) + \sum_{K \in \mathcal{C}_h} \frac{1}{\varepsilon + h_K^4} \|(g - u_h - \varepsilon \lambda_h)_+\|_{0,K}^2 \quad (3.31)$$

where $u_+ = \max\{u, 0\}$ denotes the positive part of u .

The lower bound is a simple consequence of the global versions of estimates (3.23)–(3.25). We refer to [18] for a similar consideration with more details.

Theorem 4 (A posteriori estimate – efficiency) *It holds that*

$$\eta \lesssim \|\!(u - u_h, \lambda - \lambda_h)\!\|. \quad (3.32)$$

The upper bound cannot be established as elegantly as for the second-order (membrane) obstacle problem, cf. [18], since the positive part function is not in $H^2(\Omega)$. We will use the following assumption, justified by the a priori estimate (3.27) for regular enough solution, see, e.g., [10].

Assumption 1 (Saturation assumption) *There exists $\beta < 1$ such that*

$$\|\!(u - u_{h/2}, \lambda - \lambda_{h/2})\!\|_{h/2} \leq \beta \|\!(u - u_h, \lambda - \lambda_h)\!\|_h,$$

where $(u_{h/2}, \lambda_{h/2}) \in V_{h/2} \times Q_{h/2}$ is the solution in the mesh $\mathcal{C}_{h/2}$ obtained by splitting the elements of the mesh \mathcal{C}_h .

Theorem 5 (A posteriori estimate – reliability) *It holds that*

$$\|\!(u - u_h, \lambda - \lambda_h)\!\| \lesssim \eta + S. \quad (3.33)$$

Proof Let $w \in V_{h/2}$ be the function corresponding to $(u_{h/2} - u_h, \lambda_{h/2} - \lambda_h) \in V_{h/2} \times Q_{h/2}$ in the discrete stability estimate (3.12) for which is holds, in particular, that

$$\|w\|_2 \lesssim \|\!(u_{h/2} - u_h, \lambda_{h/2} - \lambda_h)\!\|_{h/2}. \quad (3.34)$$

Let, moreover, $\tilde{w} \in V_h$ denote the Hermite type interpolant of $w \in V_{h/2}$. By scaling, one readily shows that

$$\begin{aligned} & \sum_{K \in \mathcal{C}_h} h_K^{-4} \|w - \tilde{w}\|_{0,K}^2 + \sum_{E \in \mathcal{E}_h^I} h_E^{-1} \|\nabla(w - \tilde{w})\|_{0,E}^2 \\ & + \sum_{E \in \mathcal{E}_h^I} h_E^{-3} \|w - \tilde{w}\|_{0,E}^2 \lesssim \|w\|_2^2 \quad \text{and} \quad \|\tilde{w}\|_2 \lesssim \|w\|_2. \end{aligned} \quad (3.35)$$

The discrete problem statement implies that

$$0 \leq -\mathcal{B}_h(u_h, \lambda_h; -\tilde{w}, 0) + \mathcal{L}_h(-\tilde{w}, 0). \quad (3.36)$$

From (3.12), (3.5) and (3.36) it then follows that

$$\begin{aligned} \left\| (u_{h/2} - u_h, \lambda_{h/2} - \lambda_h) \right\|_{h/2}^2 &\lesssim \mathcal{B}_{h/2}(u_{h/2} - u_h, \lambda_{h/2} - \lambda_h; w, \lambda_h - \lambda_{h/2}) \\ &\leq \mathcal{L}_{h/2}(w, \lambda_h - \lambda_{h/2}) - \mathcal{B}_{h/2}(u_h, \lambda_h; w, \lambda_h - \lambda_{h/2}) \\ &\quad - \mathcal{B}_h(u_h, \lambda_h; -\tilde{w}, 0) + \mathcal{L}_h(-\tilde{w}, 0) \\ &= (f, w - \tilde{w}) - a(u_h, w - \tilde{w}) + \langle w - \tilde{w}, \lambda_h \rangle \\ &\quad + \langle u_h + \varepsilon \lambda_h - g, \lambda_h - \lambda_{h/2} \rangle \\ &\quad + \alpha \sum_{K' \in \mathcal{C}_{h/2}} h_{K'}^4 (\mathcal{A}(u_h) - \lambda_h - f, \mathcal{A}(w))_{K'} \\ &\quad - \alpha \sum_{K' \in \mathcal{C}_{h/2}} h_{K'}^4 (\mathcal{A}(u_h) - \lambda_h - f, \lambda_h - \lambda_{h/2})_{K'} \\ &\quad - \alpha \sum_{K \in \mathcal{C}_h} h_K^4 (\mathcal{A}(u_h) - \lambda_h - f, \mathcal{A}(\tilde{w}))_K \end{aligned}$$

Using formula (3.20) to integrate by parts in $a(u_h, w - \tilde{w})$, we obtain

$$\begin{aligned} &(f, w - \tilde{w}) - a(u_h, w - \tilde{w}) + \langle w - \tilde{w}, \lambda_h \rangle \\ &= \sum_{K \in \mathcal{C}_h} (-\mathcal{A}(u_h) + \lambda_h + f, w - \tilde{w})_K \\ &\quad + \sum_{E \in \mathcal{E}_h^I} \left\{ ([M(u_h)n], \nabla(w - \tilde{w}))_E - ([Q(u_h) \cdot n], w - \tilde{w})_E \right\} \\ &= \sum_{K \in \mathcal{C}_h} (-\mathcal{A}(u_h) + \lambda_h + f, w - \tilde{w})_K \\ &\quad + \sum_{E \in \mathcal{E}_h^I} \left\{ ([M_{nn}(u_h)], \nabla(w - \tilde{w}) \cdot n)_E - ([V_n(u_h)], w - \tilde{w})_E \right\}. \end{aligned}$$

These terms are easily bounded using the Cauchy–Schwarz inequality and the interpolation estimates (3.35).

On the other hand, dividing $u_h + \varepsilon \lambda_h - g$ into its positive and negative part, we obtain the estimate

$$\begin{aligned} &\langle u_h + \varepsilon \lambda_h - g, \lambda_h - \lambda_{h/2} \rangle \\ &\leq ((u_h + \varepsilon \lambda_h - g)_+, \lambda_h) + ((u_h + \varepsilon \lambda_h - g)_-, \lambda_h - \lambda_{h/2}) \\ &\leq ((u_h + \varepsilon \lambda_h - g)_+, \lambda_h) \\ &\quad + \left(\sum_{K \in \mathcal{C}_h} \frac{1}{\varepsilon + h_K^4} \|(u_h + \varepsilon \lambda_h - g)_-\|_{0,K}^2 \right)^{1/2} \left\| (u_{h/2} - u_h, \lambda_{h/2} - \lambda_h) \right\|_{h/2} \end{aligned}$$

For the stabilising terms, we obtain the bounds

$$\begin{aligned}
& \sum_{K \in \mathcal{C}_h} h_K^4 (-\mathcal{A}(u_h) + \lambda_h + f, \mathcal{A}(\tilde{w}))_K \\
& \leq \sum_{K \in \mathcal{C}_h} h_K^4 \|\mathcal{A}(u_h) - \lambda_h - f\|_{0,K} \|\mathcal{A}(\tilde{w})\|_{0,K} \\
& \leq \left(\sum_{K \in \mathcal{C}_h} h_K^4 \|\mathcal{A}(u_h) - \lambda_h - f\|_{0,K}^2 \right)^{1/2} \left(\sum_{K \in \mathcal{C}_h} h_K^4 \|\mathcal{A}(\tilde{w})\|_{0,K}^2 \right)^{1/2} \\
& \lesssim \left(\sum_{K \in \mathcal{C}_h} h_K^4 \|\mathcal{A}(u_h) - \lambda_h - f\|_{0,K}^2 \right)^{1/2} \|w\|_2 \\
& \lesssim \left(\sum_{K \in \mathcal{C}_h} h_K^4 \|\mathcal{A}(u_h) - \lambda_h - f\|_{0,K}^2 \right)^{1/2} \|(u_{h/2} - u_h, \lambda_{h/2} - \lambda_h)\|_{h/2}, \\
& \sum_{K' \in \mathcal{C}_{h/2}} h_{K'}^4 (\mathcal{A}(u_h) - \lambda_h - f, \mathcal{A}(\tilde{w}) - (\lambda_h - \lambda_{h/2}))_{K'} \\
& \lesssim \left(\sum_{K \in \mathcal{C}_h} h_K^4 \|\mathcal{A}(u_h) - \lambda_h - f\|_{0,K}^2 \right)^{1/2} \|(u_{h/2} - u_h, \lambda_{h/2} - \lambda_h)\|_{h/2},
\end{aligned}$$

where we have used the inverse inequality (3.8) and the interpolation estimates (3.35).

The assertion follows after completing the square, using again the estimates (3.35) and (3.34) and observing that

$$\|(u - u_h, \lambda - \lambda_h)\| \leq \|(u - u_h, \lambda - \lambda_h)\|_h \leq \frac{1}{1 - \beta} \|(u_{h/2} - u_h, \lambda_{h/2} - \lambda_h)\|_{h/2}.$$

4 A practical solution algorithm

The approximation properties of the primal variable and the Lagrange multiplier are balanced when the polynomial order of the latter is four degrees smaller than that of the displacement variable, for example, when the Argyris element is coupled with a piecewise linear and discontinuous approximation of the Lagrange multiplier. It is, however, unnecessary to actually solve for the Lagrange multiplier since it can be eliminated from the stabilised formulation altogether. This approach is analogous to the derivation of Nitsche's method for Dirichlet boundary conditions (cf. [22]) and hence we refer to the proposed method as *Nitsche's method for the Kirchhoff plate obstacle problem*.

Nitsche's method can be derived in two steps. First, testing with $(0, -\mu_h)$ in the stabilised formulation (3.5), leads to the following elementwise expression for the Lagrange multiplier

$$\lambda_h|_K = \frac{1}{\varepsilon + \alpha h_K^4} (\pi_h g|_K - \pi_h u_h|_K + \alpha h_K^4 (\pi_h \mathcal{A}(u_h) - \pi_h f)|_K)_+, \quad \forall K \in \mathcal{C}_h,$$

where $\pi_h : L^2(\Omega) \rightarrow Q_h$ is the L^2 projection. Let the function $\mathcal{H} \in L^2(\Omega)$ be such that $\mathcal{H}|_K = h_K, \forall K \in \mathcal{E}_h$. Then, testing with $(v_h, 0)$, substituting the formula for λ_h in the resulting expression and choosing $Q_h = L^2(\Omega)$, gives the following nonlinear variational problem:

Problem 3 (Nitsche's method for Problem 1) Find $u_h \in V_h$ such that

$$a_h(u_h, v_h; u_h) = l_h(v_h; u_h), \quad \forall v_h \in V_h, \quad (4.1)$$

where

$$\begin{aligned} a_h(u_h, v_h; w_h) &= a(u_h, v_h) + \left(\frac{1}{\varepsilon + \alpha \mathcal{H}^4} u_h, v_h \right)_{\Omega_C(w_h)} - \left(\frac{\alpha \mathcal{H}^4}{\varepsilon + \alpha \mathcal{H}^4} \mathcal{A}(u_h), v_h \right)_{\Omega_C(w_h)} \\ &\quad - \left(\frac{\alpha \mathcal{H}^4}{\varepsilon + \alpha \mathcal{H}^4} u_h, \mathcal{A}(v_h) \right)_{\Omega_C(w_h)} - \left(\frac{\varepsilon \alpha \mathcal{H}^4}{\varepsilon + \alpha \mathcal{H}^4} \mathcal{A}(u_h), \mathcal{A}(v_h) \right)_{\Omega_C(w_h)} \\ &\quad - (\alpha \mathcal{H}^4 \mathcal{A}(u_h), \mathcal{A}(v_h))_{\Omega \setminus \Omega_C(w_h)}, \\ l_h(v_h; w_h) &= (f, v_h) + \left(\frac{1}{\varepsilon + \alpha \mathcal{H}^4} g, v_h \right)_{\Omega_C(w_h)} - \left(\frac{\alpha \mathcal{H}^4}{\varepsilon + \alpha \mathcal{H}^4} g, \mathcal{A}(v_h) \right)_{\Omega_C(w_h)} \\ &\quad - \left(\frac{\alpha \mathcal{H}^4}{\varepsilon + \alpha \mathcal{H}^4} f, v \right)_{\Omega_C(w_h)} - \left(\frac{\varepsilon \alpha \mathcal{H}^4}{\varepsilon + \alpha \mathcal{H}^4} f, \mathcal{A}(v_h) \right)_{\Omega_C(w_h)} \\ &\quad - (\alpha \mathcal{H}^4 f, \mathcal{A}(v_h))_{\Omega \setminus \Omega_C(w_h)}. \end{aligned}$$

The contact set $\Omega_C(w_h)$ above is defined as

$$\Omega_C(w_h) = \{(x, y) \in \Omega : F(w_h) > 0\},$$

with $F(w_h)$ denoting the reaction force given by

$$F(w_h) = \frac{1}{\varepsilon + \alpha \mathcal{H}^4} (g - w_h + \alpha \mathcal{H}^4 (\mathcal{A}(w_h) - f))_+.$$

The practical solution algorithm for Problem 3 is an iterative process where at each step the contact set Ω_C is approximated using the displacement field from the previous iteration so that system (4.1) becomes linear. The process is terminated as soon as the norm of the displacement field is below a predetermined tolerance $TOL > 0$. The stopping criterion is formulated with respect to the strain energy norm

$$\|w\|_E = \sqrt{a(w, w)}. \quad (4.2)$$

Algorithm 1 Nitsche's method, with contact iterations

- 1: $k \leftarrow 0$
 - 2: **while** $k < 1$ or $\|u_h^k - u_h^{k-1}\|_E \leq TOL$ **do**
 - 3: Find $u_h^{k+1} \in V_h$ s.t. $a_h(u_h^{k+1}, v_h; u_h^k) = l_h(v_h; u_h^k), \forall v_h \in V_h$.
 - 4: $k \leftarrow k + 1$
 - 5: **end while**
 - 6: **return** u_h^k
-

For a discussion regarding the convergence of iterations in Algorithm 1, we refer to [18] where we compare this approach to the semismooth Newton method for solving a stabilised second-order obstacle problem. We point out that the semismooth Newton method (see e.g. [26]) corresponds to an algorithm, similar to Algorithm 1, where the contact area follows element boundaries. Hence, we expect Algorithm 1 to behave numerically as a semismooth Newton-type strategy applied to variational inequalities.

For an adaptive refinement, we use the maximum strategy with the parameter $\theta \in (0, 1)$ for marking and the red-green-blue refinement, see e.g. [25, 2]. The error estimator is defined as

$$\mathcal{E}_K^2 = \eta_K^2 + \frac{1}{2} \sum_{E \subset K} \eta_E^2 + ((u_h - g + \varepsilon \lambda_h)_+, \lambda_h)_K + S_{K,\varepsilon}^2, \quad (4.3)$$

where

$$S_{K,\varepsilon} = \frac{1}{\sqrt{\varepsilon + h_K^4}} \|(g - u_h - \varepsilon \lambda_h)_+\|_{0,K} \quad (4.4)$$

Given the displacement field u_h , the reaction force $\lambda_h = F(u_h)$ is computed as indicated in Problem 3. We start with an initial mesh \mathcal{C}_h^0 and terminate the computation after a predetermined number of adaptive refinement steps M . The resulting procedure is summarised in the listing Algorithm 2.

Algorithm 2 The adaptive Nitsche's method

- 1: $j \leftarrow 0$
- 2: **while** $j < M$ **do**
- 3: Solve u_h^{j+1} using Algorithm 1 and the mesh \mathcal{C}_h^j .
- 4: Evaluate the error estimator \mathcal{E}_K for every $K \in \mathcal{C}_h^j$.
- 5: Using the red-green-blue refinement strategy [25, 2], construct \mathcal{C}_h^{j+1} by refining the elements K that satisfy the inequality

$$\mathcal{E}_K > \theta \max_{K' \in \mathcal{C}_h^j} \mathcal{E}_{K'}.$$

- 6: $j \leftarrow j + 1$
 - 7: **end while**
-

5 Numerical results

We illustrate the performance of the proposed algorithms by solving two example problems and comparing the uniform and adaptive meshing. The adaptive method is expected to recover the optimal rate of convergence with respect to the number of degrees of freedom N , i.e.

$$\|(u - u_h, \lambda - \lambda_h)\| \propto N^{-\frac{k-1}{2}},$$

where k is the polynomial order of the finite element basis. As a measure of error we use the global estimator $\eta + S$. We expect that, asymptotically, it holds

$$\| (u - u_h, \lambda - \lambda_h) \| \propto \eta + S.$$

Let $\Omega = [0, 1]^2$ and let \mathcal{C}_h be a triangulation of Ω . The finite element space for the displacement field consists of a set of piecewise polynomials of order five, i.e.

$$V_h = \{w \in H_0^2(\Omega) : w|_K \in P_5(K) \forall K \in \mathcal{C}_h\}.$$

The global C^1 -continuity is conceived by implementing the Argyris basis functions, c.f. [11]. In both examples, the loading function and the material parameters are chosen as $f = -10$, $d = 1$, $E = 1$ and $\nu = 0$. For the parameters α , TOL and θ , we use the values $\alpha = 10^{-5}$, $TOL = 10^{-10}$ and $\theta = 0.5$. In each case, we start with the mesh shown in the upper left panel of Figure 5.1 and apply either a uniform refinement (each triangle is split into four subtriangles) or Algorithm 2 with $M = 5$.

The first example is that of a rigid obstacle, $\varepsilon = 0$, with its shape defined by

$$g(x, y) = -100((x - 0.5)^2 + (y - 0.5)^2). \quad (5.1)$$

This obstacle is smooth and hence it belongs to $H^2(\Omega)$ as required by the continuous formulation. Nevertheless, its shape is sharp due to the moderately large negative coefficient. Qualitatively, the plate behaves subject to this type of obstacle as it would under a point load and we expect the error estimator to be large near the midpoint $(0.5; 0.5)$.

The resulting sequence of adaptive meshes is depicted in Figure 5.1 and the respective global errors can be found in Figure 5.2. The discrete solution and the Lagrange multiplier, after three adaptive refinements, are shown in Figures 5.4(A) and 5.5(A). The discrete functions are visualised in a refined mesh as they may have high-order and non-smooth variations inside the elements. The results of Figure 5.2 clearly indicate that the adaptive method gains the optimal rate of convergence $\mathcal{O}(N^{-2})$ whereas the uniform refinement is observed to be $\mathcal{O}(N^{-1/2})$. Note that if the numerical contact region was larger, for example using a less sharp obstacle, the convergence rate would become limited by the regularity of the solution, i.e. with uniform refinement eventually by $\mathcal{O}(N^{-3/4})$.

In the second example, we consider an elastic obstacle ($\varepsilon > 0$) defined by the function

$$g(x, y) = \begin{cases} 0, & \text{if } (x, y) \in [0.3; 0.7]^2, \\ -1, & \text{otherwise.} \end{cases} \quad (5.2)$$

Note that $g \in L^2(\Omega)$ but $g \notin H^1(\Omega)$. Computing the cases $\varepsilon = 10^{-j}$, $j \in \{3, 4, 5, 6\}$, we observe that the behaviour of the reaction force varies quite much from case to case as revealed by the discrete Lagrange multipliers depicted in Figure 5.5 and by the discrete contact sets shown in Figure 5.6. In particular, the contact sets corresponding to less rigid obstacles remain simply connected which is not the case for the stiffer obstacles.

The resulting error graphs for the adaptive and uniform refinements can be found in Figure 5.3. The sequences of adaptive meshes can be found in Figures 5.7–5.10.

We observe that for uniform refinements the slope of the error graph is getting worse when the obstacle is stiffened and that the adaptive meshing strategy successfully recovers the optimal rate of convergence $\mathcal{O}(N^{-2})$, independently of the value of ε .

References

1. Aleksanyan, G.: Regularity of the free boundary in the biharmonic obstacle problem. arXiv preprint:1603.06819
2. Bartels, S.: Numerical Methods for Nonlinear Partial Differential Equations, *Springer Series in Computational Mathematics*, vol. 47. Springer (2015)
3. Blum, H., Rannacher, R.: On the boundary value problem of the biharmonic operator on domains with angular corners. *Math. Meth. Appl. Sci.* **2**, 556–581 (1980)
4. Brenner, S., Gedicke, J., Sung, L.y., Zhang, Y.: An a posteriori analysis of C^0 interior penalty methods for the obstacle problem of clamped Kirchhoff plates. *SIAM J. Numer. Anal.* **55**(1), 87–108 (2017)
5. Brenner, S., Sung, L.y., Zhang, H., Zhang, Y.: A quadratic C^0 interior penalty method for the displacement obstacle problem of clamped Kirchhoff plates. *SIAM J. Numer. Anal.* **50**(6), 3329–3350 (2012)
6. Brenner, S., Sung, L.y., Zhang, H., Zhang, Y.: A Morley finite element method for the displacement obstacle problem of clamped Kirchhoff plates. *J. Comput. Appl. Math.* **254**, 31–42 (2013)
7. Brenner, S., Sung, L.y., Zhang, Y.: Finite element methods for the displacement obstacle problem of clamped plates. *Math. Comp.* **81**(279), 1247–1262 (2012)
8. Brezzi, F., Hager, W.W., Raviart, P.A.: Error estimates for the finite element solution of variational inequalities. II. Mixed methods. *Numer. Math.* **31**(1), 1–16 (1978/79)
9. Caffarelli, L.A., Friedman, A.: The obstacle problem for the biharmonic operator. *Ann. Sc. Norm. Super. Pisa Cl. Sci.* (5) **6**(1), 151–183 (1979)
10. Chouly, F., Fabre, M., Hild, P., Pousin, J., Renard, Y.: Residual-based a posteriori error estimation for contact problems approximated by Nitsche’s method. *IMA J. Numer. Anal.* **38**(2), 921–954 (2018)
11. Ciarlet, P.G.: *The Finite Element Method for Elliptic Problems*. North-Holland (1978)
12. Feng, K., Shi, Z.C.: *Mathematical Theory of Elastic Structures*. Springer-Verlag, Berlin; Science Press, Beijing (1996)
13. Frehse, J.: Zum Differenzierbarkeitsproblem bei Variationsungleichungen höherer Ordnung. *Abh. Math. Sem. Univ. Hamburg* **36**(1), 140–149 (1971)
14. Fusciardi, A., Scarpini, F.: A mixed finite element solution of some biharmonic unilateral problem. *Numer. Funct. Anal. Optim.* **2**(5), 397–420 (1980)
15. Glowinski, R., Marini, L.D., Vidrascu, M.: Finite-element approximations and iterative solutions of a fourth-order elliptic variational inequality. *IMA J. Numer. Anal.* **4**(2), 127–167 (1984)
16. Gudi, T.: A new error analysis for discontinuous finite element methods for linear elliptic problems. *Math. Comp.* **79**(272), 2169–2189 (2010)
17. Gudi, T., Porwal, K.: A C^0 interior penalty method for a fourth-order variational inequality of the second kind. *Numer. Methods Partial Differ. Equ.* **32**(1), 36–59 (2016)
18. Gustafsson, T., Stenberg, R., Videman, J.: Mixed and stabilized finite element methods for the obstacle problem. *SIAM J. Numer. Anal.* **55**(6), 2718–2744 (2017)
19. Gustafsson, T., Stenberg, R., Videman, J.: A posteriori estimates for conforming Kirchhoff plate elements. *SIAM J. Sci. Comput.* **40**(3), A1386–A1407 (2018)
20. Han, W., Hua, D., Wang, L.: Nonconforming finite element methods for a clamped plate with elastic unilateral obstacle. *J. Integral Equations Appl.* **18**(2), 267–284 (2006)
21. Scholz, R.: Mixed finite element approximation of a fourth order variational inequality by the penalty method. *Numer. Funct. Anal. Optim.* **9**, 233–247 (1987)
22. Stenberg, R.: On some techniques for approximating boundary conditions in the finite element method. *J. Comput. Appl. Math.* **63**(1-3), 139–148 (1995)
23. Stenberg, R., Videman, J.: On the error analysis of stabilized finite element methods for the Stokes problem. *SIAM J. Numer. Anal.* **53**, 2626–2633 (2015)
24. Tosone, C., Maceri, A.: The clamped plate with elastic unilateral obstacles: a finite element approach. *Math. Models Methods Appl. Sci.* **13**, 1231–1243 (2003)
25. Verfürth, R.: *A Posteriori Error Estimation Techniques for Finite Element Methods*. Numerical Mathematics and Scientific Computation. Oxford University Press, Oxford (2013)
26. Wohlmuth, B.: Variationally consistent discretization schemes and numerical algorithms for contact problems. *Acta Numerica* **20**, 569–734 (2011)

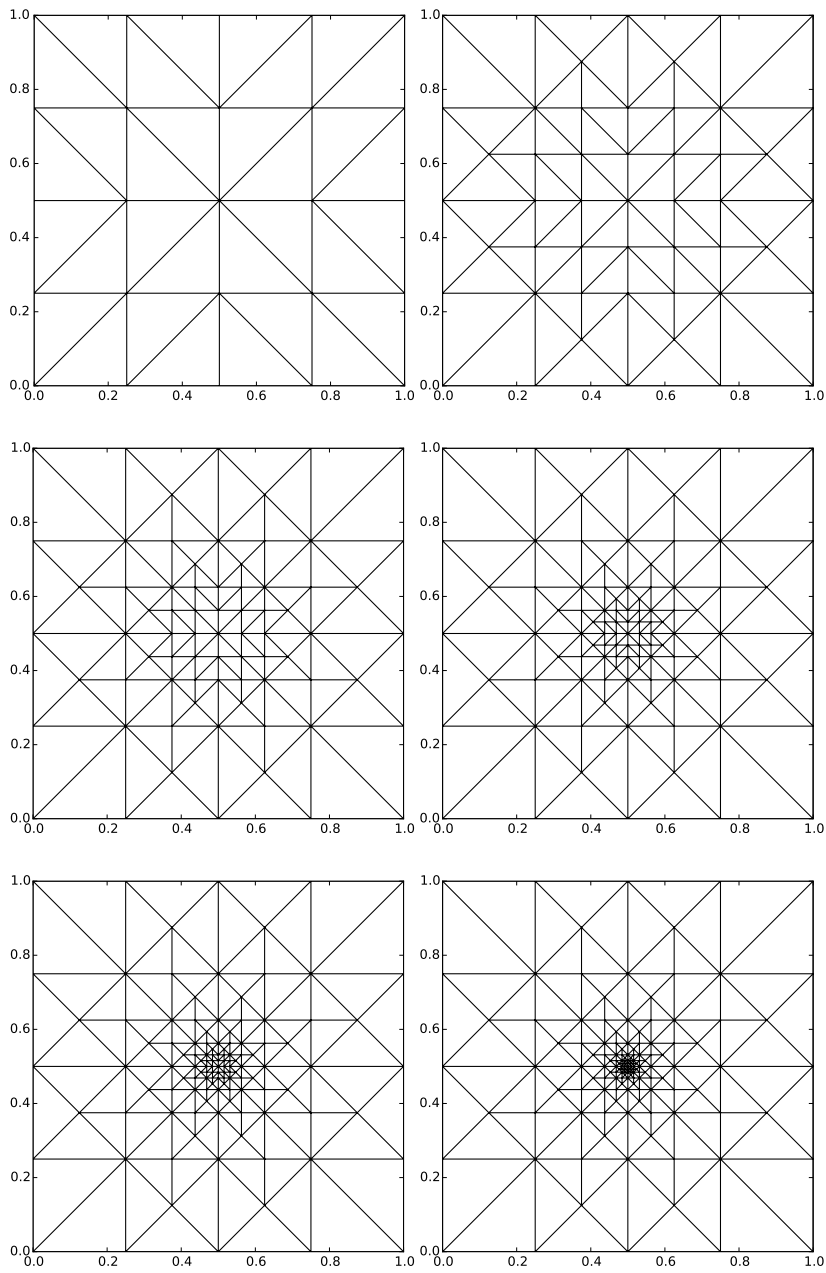


Fig. 5.1: The sequence of adaptive meshes in the rigid obstacle case.

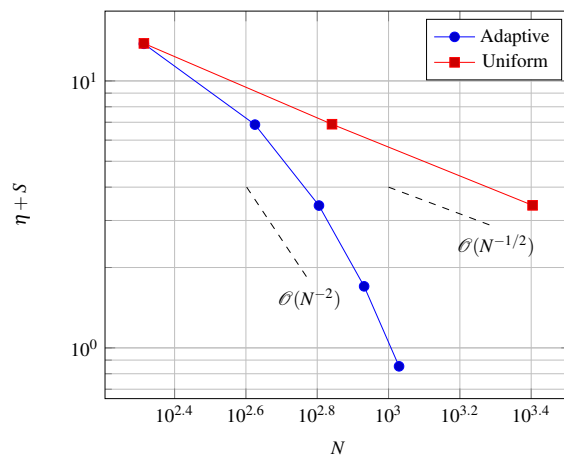


Fig. 5.2: The global error estimator, plotted as a function of the number of degrees of freedom N , in the rigid obstacle case. The optimal rate of convergence for the Argyris element, $\mathcal{O}(N^{-2})$, is obtained by the adaptive meshing strategy. The regularity of the exact solution limits the convergence rate in uniform refinement.

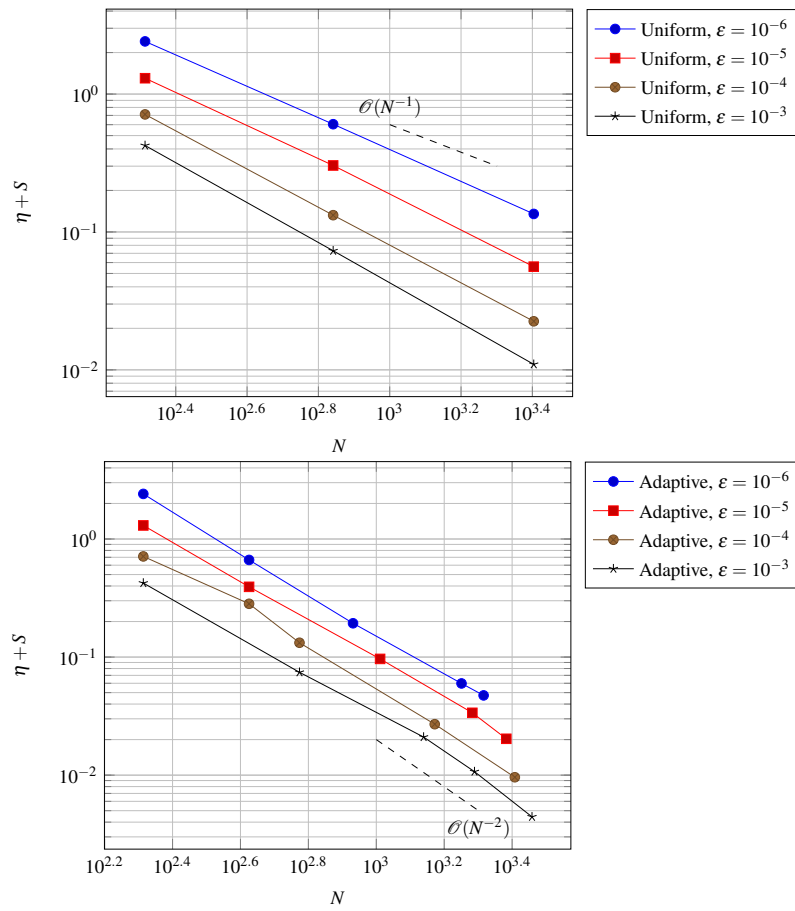


Fig. 5.3: The global error estimator in the elastic case plotted as a function of the number of degrees of freedom N . The upper and lower diagrams correspond to the uniform and the adaptive refinements, respectively.

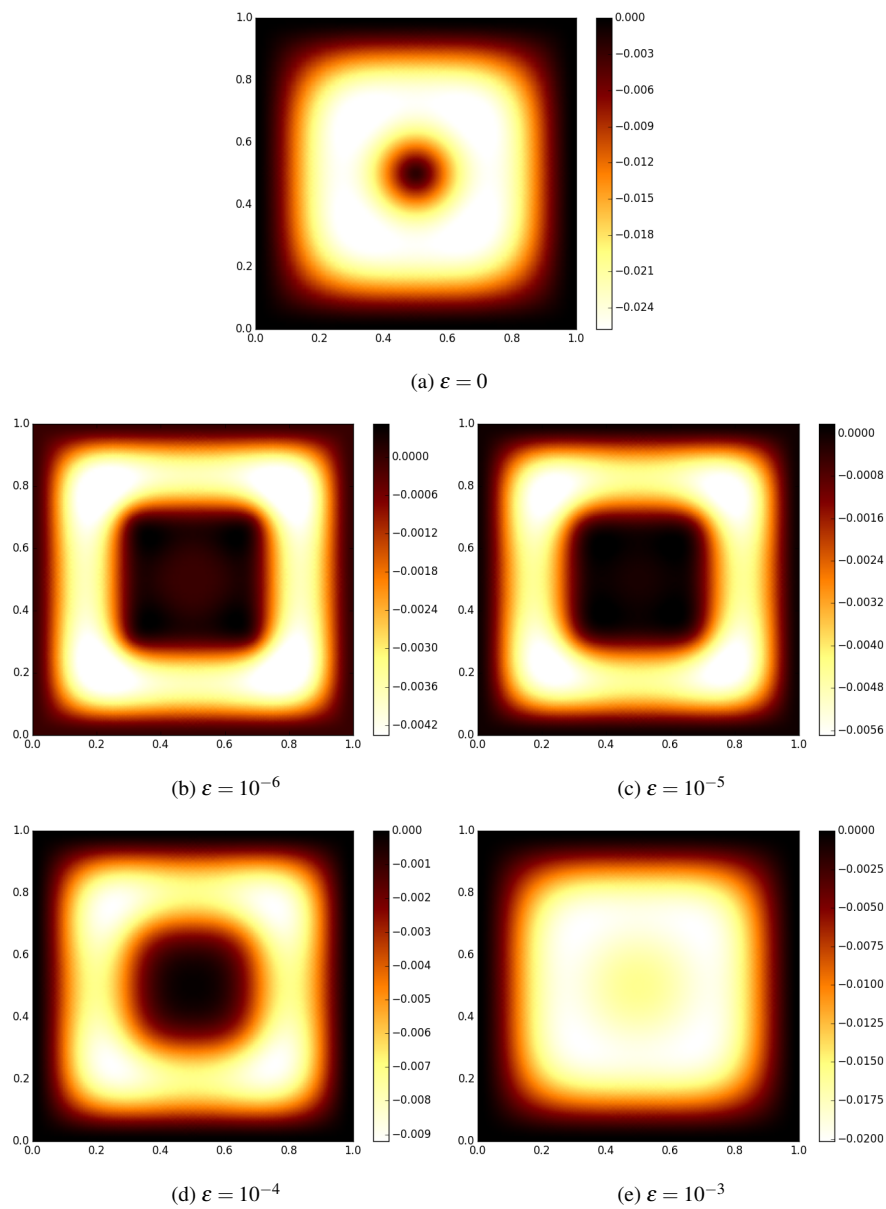


Fig. 5.4: The discrete displacements shown for five different values of ϵ after three adaptive refinements in each case. Note that the solutions are visualised on a more refined mesh.

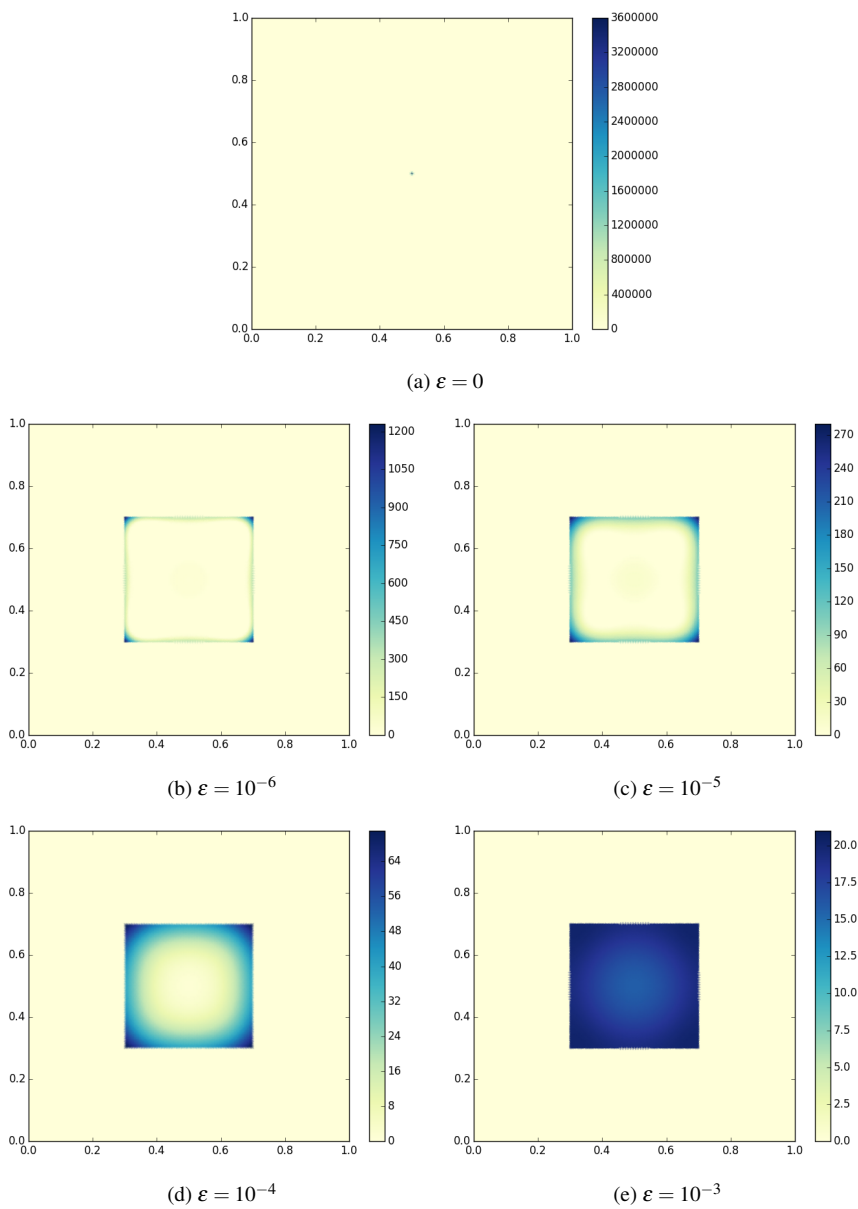


Fig. 5.5: The discrete Lagrange multipliers shown for five different values of ε after three adaptive refinements in each case. Note that the solutions are visualised on a more refined mesh.

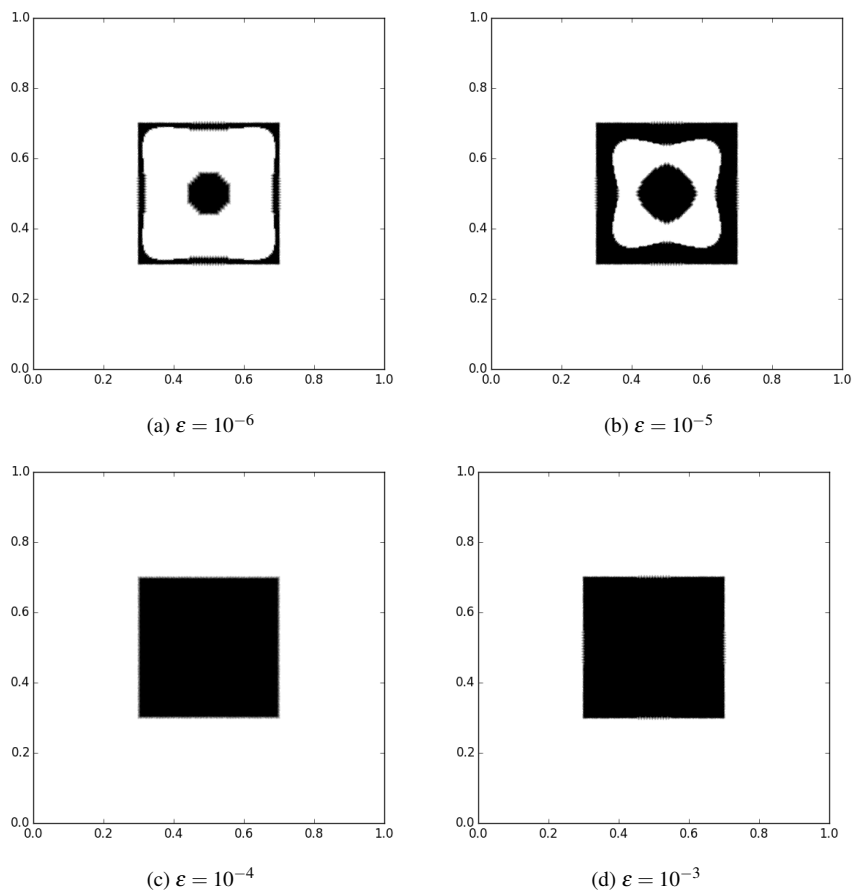


Fig. 5.6: The approximate contact sets (i.e. the regions where the discrete Lagrange multipliers are positive) after three adaptive refinements in each of the cases.

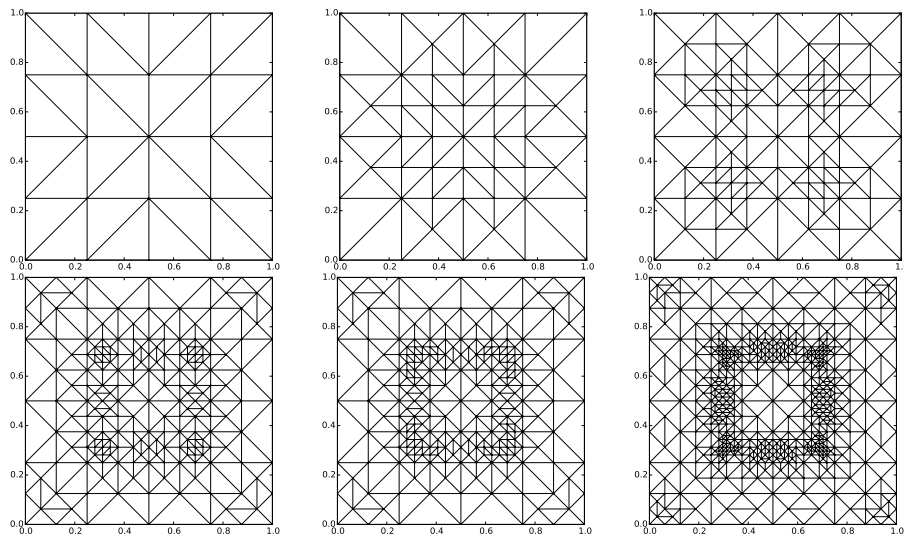


Fig. 5.7: The sequence of adaptive meshes in the elastic obstacle case with $\varepsilon = 10^{-6}$.

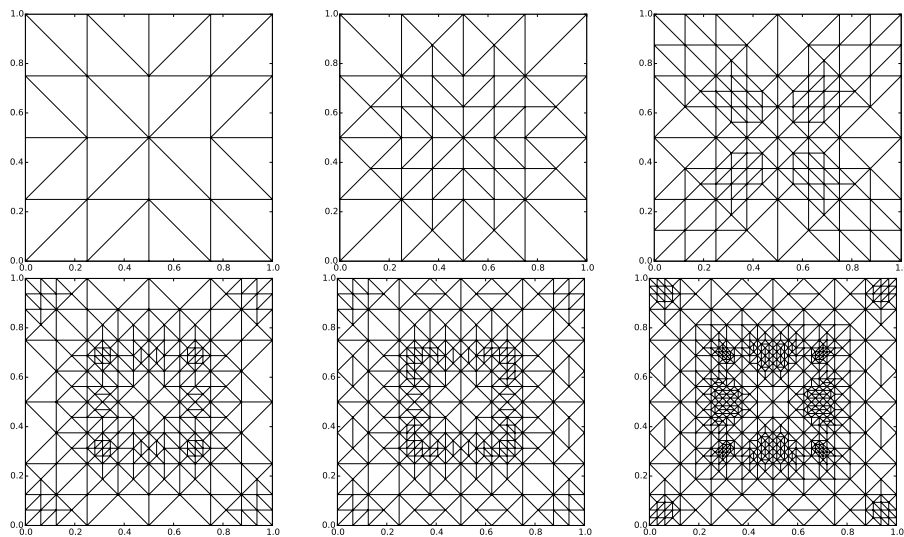


Fig. 5.8: The sequence of adaptive meshes in the elastic obstacle case with $\varepsilon = 10^{-5}$.

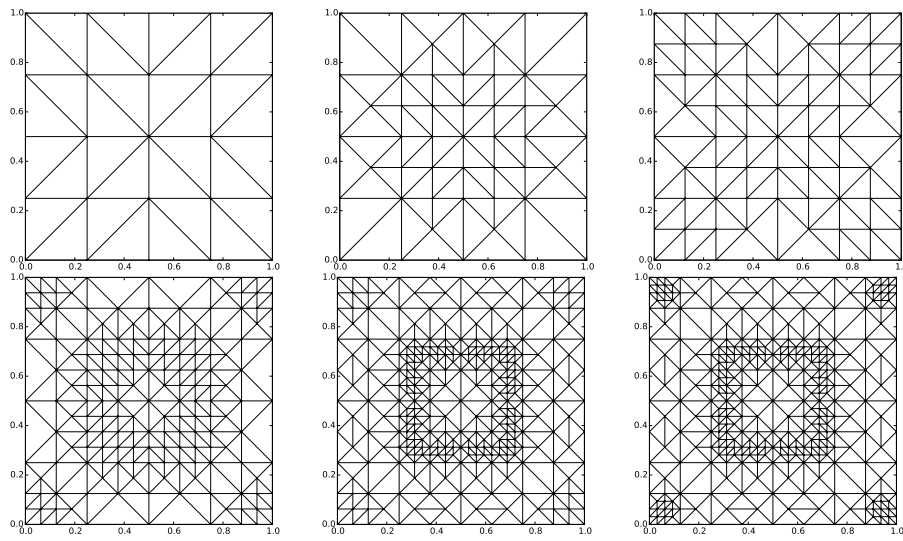


Fig. 5.9: The sequence of adaptive meshes in the elastic obstacle case with $\varepsilon = 10^{-4}$.

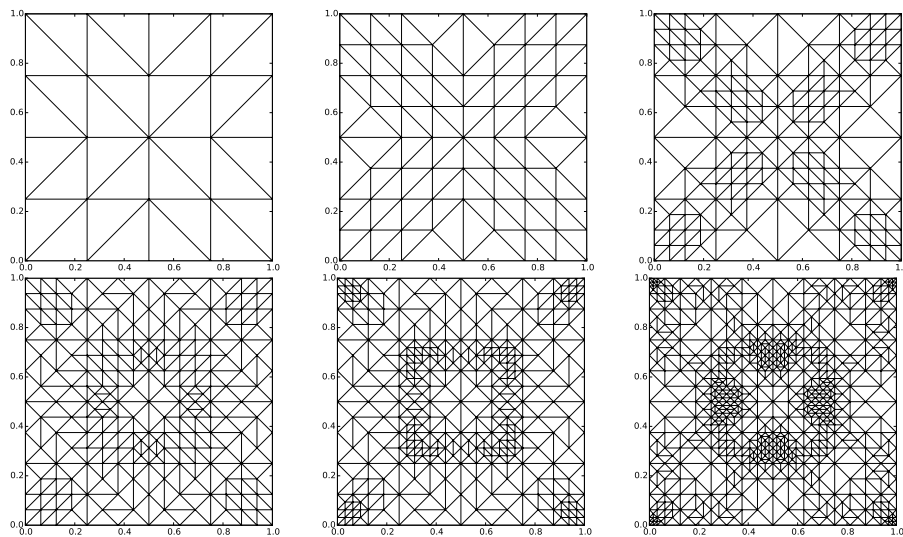


Fig. 5.10: The sequence of adaptive meshes in the elastic obstacle case with $\varepsilon = 10^{-3}$.